Title
STRESSED MIRROR POLISHING: A TECHNIQUE FOR PRODUCING NON-AXISYMMETRIC MIRRORS

Author
Lubliner, J.

Publication Date
1979-12-01

Lawrence Berkeley Laboratory
UNIVERSITY OF CALIFORNIA

Physics, Computer Science & Mathematics Division

Submitted to Applied Optics

STRESSED MIRROR POLISHING: A TECHNIQUE FOR PRODUCING NON-AXISYMMETRIC MIRRORS

Jacob Lubliner and Jerry Nelson

December 1979

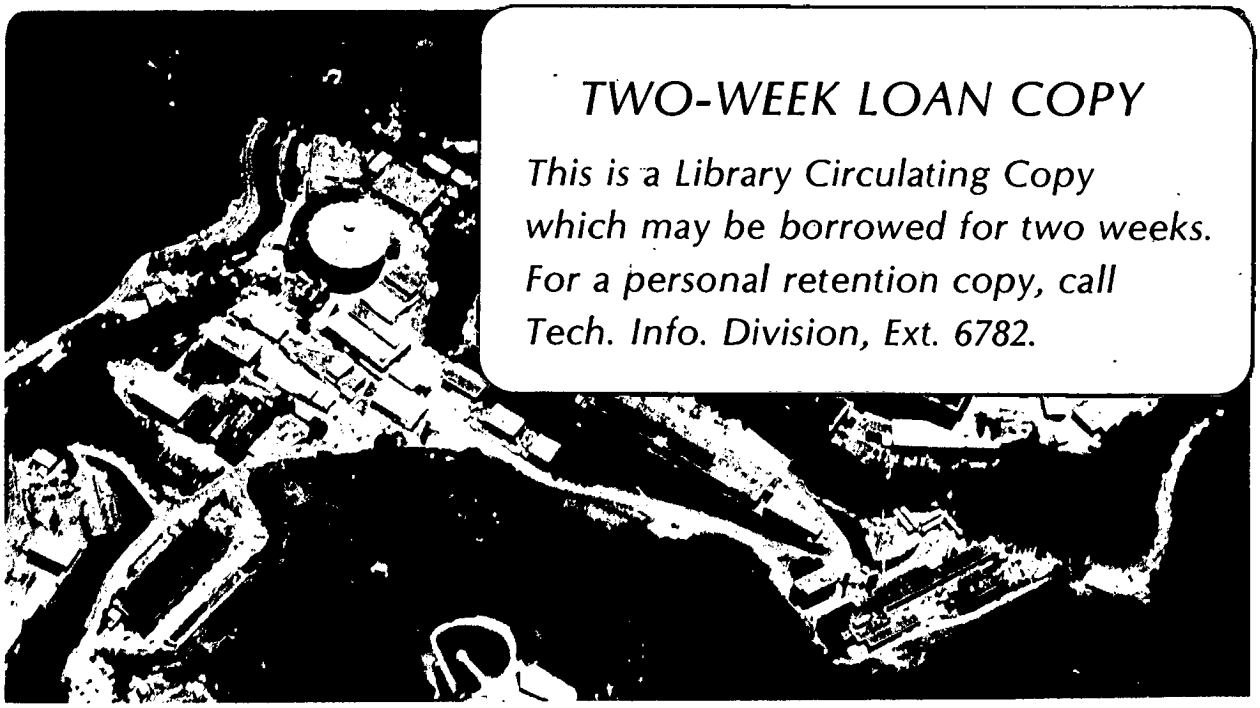

Prepared for the U.S. Department of Energy under Contract W-7405-ENG-48

DISCLAIMER

LBL#9967

STRESSED MIRROR POLISHING:

A TECHNIQUE FOR PRODUCING NON-AXISYMMETRIC MIRRORS

by

Jacob Lubliner and Jerry Nelson

Abstract

The theoretical basis is developed for a technique to fabricate non-axisymmetric mirrors. Stresses are applied to a mirror blank which would have the effect of elastically deforming a desired surface into a sphere. A sphere is then polished into the blank, and upon release of the applied stress, the spherical surface deforms into the desired one. The method can be applied iteratively, so arbitrary accuracy should be possible. Calculations of the stresses and deformations are carried out in detail for an off-axis section of a paraboloid. For a very general class of surfaces, it is sufficient to only impose appropriate stresses at the edge of the blank plus a uniform pressure on the back.

1. Introduction

The fabrication of high-quality non-axisymmetric optical surfaces has traditionally been vastly more difficult than producing axisymmetric surfaces. Among the axisymmetric surfaces, the sphere is the easiest to fabricate, with commonly desired surfaces such as paraboloids and hyperboloids being substantially more difficult. Even with the advances in computer-controlled polishing, made by some of the large optical firms, non-axisymmetric surfaces are a challenging task, one very much more difficult than polishing spheres.

The University of California is currently designing a 10-meter optical ground-based telescope[1], and one of the designs being considered is based on a segmented primary mirror of either parabolic or hyperbolic shape[2,3,4]. The primary is expected to be about f/2. The segments are hexagonal in outline, 1.4 m in diameter and 10 cm thick. These mirror segments must be off-axis sections of a paraboloid, and the entire set of 60 must be made to conform to a single paraboloidal surface. Because of the great difficulty in making even a single off-axis paraboloid by traditional methods, the construction of a matched set of 60 mirrors appears quite formidable. Our desire to produce these mirrors accurately, quickly, and economically was the impetus for developing the technique described in this paper.

In general, the idea is to apply an appropriate set of forces to a mirror blank such that after a sphere has been ground and polished into the blank, the forces can be removed and the polished spherical surface will deform elastically into the desired non-axisymmetric surface. So long as the material behaves elastically, with no hysteresis, and the desired surface is smooth, there will exist a force function capable of producing the desired deformation. Thus, in principle, one can reduce the difficulty of polishing

non-axisymmetric mirrors to the much simpler task of polishing spheres. We show in this paper how for circular mirrors of uniform thickness, a very general class of surfaces can be created by an extremely simple force distribution. (In a companion paper[5] we describe the fabrication of an off-axis section of a paraboloid using this technique.)

Historically, this general idea was first used by Bernard Schmidt in making an axisymmetric correcting lens for a Schmidt telescope, and the theory and method for this technique is described by Everhart[6]. An interesting variant of the idea we develop in this article is described by LeMaitre[7], where variations in plate thickness are deliberately introduced to attempt to achieve a set of desired deflections under external loads. A related idea, that of bending a given mirror into another shape by the use of a warping harness to adjust astigmatism has been described by Leonard[8] and Alvarez[9]. In these applications, no polishing during warping was attempted; rather, the warping harness was a permanent part of the desired mirror.

It is well known that any continuous function defined in a region of the x-y plane can be represented by a double power series in x and y. If the region is a circle of radius a about the origin, then it is convenient to use polar coordinates (ρ,θ), where $\rho = r/a$, $r = \sqrt{x^2+y^2}$, and $\theta = \tan^{-1}(y/x)$. It can be shown that the series then takes the form

$$\sum_{m=0}^{\infty} \sum_{\substack{n=0, \\ m-n \text{ even}}}^{m} (\alpha_{mn}\cos n\theta + \beta_{mn}\sin n\theta)\rho^m \qquad (1.1)$$

By means of elastic plate theory it can further be shown that the proper application of bending moments and shearing forces around the periphery of a flat plate, plus a uniform or linearly varying pressure on the back of the plate (as might be exerted by an elastic support pad), will deflect the plate into any surface given by a function described by (1.1), with the restriction that for $m \geq 6$, the only non-vanishing coefficients α_{mn} and β_{mn}

are those with m = n and m = n + 2. Even with this restriction, equation (1.1) still describes all commonly produced optical surfaces.

The material should behave elastically for this procedure, so some materials may not be suitable for this technique; but at least one material, glass, is known to have nearly ideal elastic properties[10]. If the material responds linearly to the imposed forces, the resulting deflections are independent of the internal stresses of the original blank and of changes in the internally generated stresses caused by grinding and polishing.

An attractive feature of the technique is the ability to produce the desired surface iteratively. If the applied forces are only approximately correct, due to approximations in the theory, incomplete knowledge of the blank's elastic properties, or systematic errors in the application of the desired forces, the surface produced will not match the desired one. Measurements of the errors in the fabricated surface can then be used to calculate corrective forces, which when reapplied along with the original set of forces can be used as the basis for a second spherical polish and test cycle and so on. Thus if the results of a single polish contain errors of order ε_o and the desired deflection is of order d, one can expect the error after n polish cycles to be

$$\varepsilon_n \sim (\frac{\varepsilon_0}{d})^n d$$

If $\varepsilon_o/d < 1$ the technique converges to produce the desired surface. In practice, ε_o/d is of order 10^{-2} and accurate convergence to the desired surface is achieved in 2 or 3 polishings. Appreciable changes in the thickness of the blank from the grinding and polishing will of course affect the deflections caused by the applied forces, but in a predictable fashion. In practice these changes are small and do not strongly affect the convergence of polishing iterations.

Since this technique was motivated by the U. C. telescope project we use as examples here sections of a mirror with a 40-meter radius of curvature and we assume a paraboloidal surface. We begin the development of the theory with a derivation of the equations describing the surfaces involved. The following section discusses the deflections of circular plates and establishes the force system needed to obtain the desired deflections. Section 4 discusses the stresses imposed on the plate and thus establishes what surfaces are actually possible without breaking or otherwise exceeding the elastic limit of the mirror blank. The derivation of the results used in Sections 3 and 4 is shown in an appendix.

2. Geometry

In this section we will derive the expression for the deflection representing the difference between a sphere and an off-axis section of a paraboloid. In a global cartesian coordinate system (X,Y,Z), a paraboloid of revolution about the Z-axis, with a focal length $f = k/2$ (so that k is the radius of curvature at the vertex), is described by

$$Z = \frac{X^2 + Y^2}{2k} . \tag{2.1}$$

Let P denote a point on the paraboloid located at a distance R from the Z-axis; the coordinates of P are $(R, 0, R^2/2k)$. We wish to transform equation (2.1) into a local coordinate system (x, y, z) whose origin is at P, such that the x-y plane is tangent to the paraboloid. We may, for convenience, let $y = Y$. The inclination of the x-y plane with respect to the X-Y plane is $\phi = \tan^{-1}\varepsilon$, where $\varepsilon = R/k$. The geometry is illustrated in Figure 1.

For convenience, we denote $\cos\phi$ and $\sin\phi$ by c and s. Then the coordinate systems (X,Y,Z) and (x,y,z) are related by

$$X = R + cx - sz,$$

$$Y = y,$$

$$Z = (R^2/2k) + cz + sx.$$

With these expressions inserted in equation (2.1), this equation becomes

$$\frac{R^2}{2k} + cz + sx = \frac{1}{2k}[(R + cx - sz)^2 + y^2].$$

Expanding and rearranging, we can write this in the form of a quadratic equation in z:

$$cs^2z^2 - 2(k + c^2sx)z + c(c^2x^2 + y^2) = 0$$

where R is eliminated by means of the identities $sR + ck = k/c$

and $cR = sk$. When the quadratic equation is solved for z, then the solution which satisfies the condition that $z = 0$ when $x = y = 0$ is

$$z = \frac{1}{cs^2}(k + c^2sx - \sqrt{k^2 + 2c^2skx - c^2s^2y^2}). \tag{2.2}$$

We expand the right-hand side of this equation in a power series, obtaining

$$z = \frac{c}{2k}(c^2x^2 + y^2) - \frac{c^3s}{2k^2}x(c^2x^2 + y^2) + \frac{c^3s^2}{8k^3}(c^2x^2 + y^2)(5c^2x^2 + y^2) + O(\varepsilon^3r^5/k^4), \tag{2.3}$$

where $r = \sqrt{x^2 + y^2}$. If the radius of the plate is a, then the largest neglected term is of order $\varepsilon^3a^5/k^4 = R^3a^5/k^7$.

Now consider a sphere of radius ℓ, centered at an arbitrary point with local coordinates $(x_o, 0, z_o)$; this is described explicitly by

$$z = z_o - \sqrt{\ell^2 - y^2 - (x - x_o)^2},$$

or, in a power-series expansion,

$$z = (z_o - \sqrt{\ell^2 - x_o^2}) - (\frac{x_o}{\ell} + \frac{x_o^3}{2\ell^3})x + \frac{r^2}{2\ell} + \frac{x_o^2}{4\ell^3}(3x^2 + y^2) - \frac{x_o x r^2}{2\ell^3} + \frac{r^2}{8\ell^3} + O(\frac{x_o r^5}{\ell^5}, \frac{r^6}{\ell^5}). \tag{2.4}$$

The goal of this study is to produce, by means of applied loads, <u>elastic</u> displacements w equal to the difference between the right-hand sides of equations (2.3) and (2.4). However, the constant and linear terms in equation (2.4) represent <u>rigid-body</u> displacements and are therefore of no interest. Consequently we let $x_o = 0$ and $z_o = \ell$ (that is, we consider only tangent spheres at P), and equation (2.4) simplifies to

$$z = \frac{r^2}{2\ell} + \frac{r^4}{8\ell^3} + O(r^6/\ell^5). \tag{2.5}$$

If z_{par} and z_{sph} denote z as given by equations (2.3) and (2.5) respectively, and if w is defined as $z_{sph} - z_{par}$, then the power-series expansion for w takes the following form when transformed into the dimensionless polar coordinates (ρ,θ):

$$w = \alpha_{20}\rho^2 + \alpha_{22}\rho^2\cos 2\theta + \alpha_{31}\rho^3\cos\theta + \alpha_{33}\rho^3\cos 3\theta + \alpha_{40}\rho^4 + \alpha_{42}\rho^4\cos 2\theta + \text{neglected terms.} \qquad (2.6)$$

The coefficients α_{mn} are given in terms of a, k, ℓ and ε as follows:

$$\alpha_{20} = \frac{a^2}{2k}\left(\frac{k}{\ell} - 1 + \varepsilon^2 + \frac{9}{8}\varepsilon^4 + \frac{5}{4}\varepsilon^6 + \ldots\right), \qquad \text{focus}$$

$$\alpha_{22} = \frac{a^2}{4k}\varepsilon^2\left(1 - \frac{3}{2}\varepsilon^2 + \frac{15}{8}\varepsilon^4 + \ldots\ldots\right), \qquad \text{astigmatism}$$

$$\alpha_{31} = (a^3/2k^2)\varepsilon\left(1 - \frac{11}{4}\varepsilon^2 + \frac{21}{4}\varepsilon^4 + \ldots\right), \qquad \text{coma}$$

$$\alpha_{33} = -(a^3/8k^2)\varepsilon^3(1 - 3\varepsilon^2 + 6\varepsilon^4 + \ldots\ldots),$$

$$\alpha_{40} = (a^4/8k^3)\left[\left(\frac{k}{\ell}\right)^3 - 3\varepsilon^2(1 - 4\varepsilon^2 + \ldots)\right], \qquad \text{spherical aberration}$$

$$\alpha_{42} = -(a^4/4k^3)\varepsilon^2(1 - 5\varepsilon^2 + \ldots\ldots).$$

Note that in each coefficient α_{mn}, the leading term is of order $(a^m/k^{m-1})\varepsilon^n$. Since both R and a are small compared to k, it can be seen that the largest of the neglected terms of (2.6) are those whose coefficients are α_{60}, α_{53} and α_{44}, of order a^6/k^5, $(a^5/k^4)\varepsilon^3$ and $(a^4/k^3)\varepsilon^4$, respectively. For mirror segments with a = 0.7 m, k = 40 m and R $\leq$ 5 m, these quantities are no greater than about a millimicron and therefore completely negligible.

The sphere radius may be chosen so as to minimize the rms value of the deflection described by equation (2.6). A close approximation to this radius can be shown to be

$$\ell = \ell_o\left(1 + \frac{a^2}{4\ell_o^2}\right), \qquad (2.7)$$

where $\ell_o = 2k/(c + c^3)$. With this value of ℓ, and with the values of a and k as above, the values of the coefficients α_{20}, ..., α_{42} are plotted against the off-axis distance R in Figure 2.

3. Plate Bending

The determination of the forces necessary to produce a given deflection pattern in a glass plate constitutes a straight-forward problem in elastic plate theory, since glass is nearly perfectly linearly elastic at sufficiently low stresses. The deflection w of a uniform, linearly and isotropically elastic, thin plate is governed by the partial differential equation

$$D\nabla^4 w = q,$$

where q is the transverse load per unit area (measured as positive in the same direction as the deflection); ∇^4 is the operator $(\partial^2/\partial x^2 + \partial^2/\partial y^2)^2$ (where x and y are cartesian coordinates in the plane of the plate); and $D = Eh^3/12(1-\nu^2)$, where h is the plate thickness while E and ν are respectively, the Young's modulus and Poisson's ratio of the glass.

The desired deflection given by equation (2.6) may be produced by a combination of bending moments and shearing forces around the edge and uniform transverse loading (see Fig. 3). Since a uniform transverse load produces no tilting moment, the edge moment and shear distributions must be in moment equilibrium. It is possible to eliminate this constraint, and permit arbitrary moment and shear distribution around the edge, by permitting the transverse loading to vary linearly over the plate surface, that is,

$$q = q_o + q_1 x + q_2 y . \qquad (3.1)$$

This kind of loading may be achieved by supporting the plate on a rubber pad which in turn rests on a flat rigid base. If the rubber pad behaves like a Winkler foundation[11], then the pressure it will exert at every point will be proportional to the displacement of the plate at that point. Since the rubber is considerably softer than the glass, the bending

displacements of the plate will be negligible compared to its rigid-body displacements. Consequently a transverse pressure of the form (3.1) may be reasonably expected.

For loadings given by equation (3.1) there exists a theory of moderately thick plates, due to Love[12], which is more exact than the classical (thin-plate) theory. The theories are discussed in the Appendix. In what follows, we present the equations resulting from the Love theory which govern the relation between, on the one hand, deflection, and on the other hand, bending moment and shearing force around the circumference of a circular plate of radius a.

3.1 Deflections

The most general top-surface deflection corresponding to an arbitrary distribution of bending moment and shearing force around the circumference, together with a transverse upward loading on the bottom surface described by (3.1) is given by the following equation:

$$w(\rho,\theta) = \sum_{n=0}^{\infty} \left[(\alpha_{nn}\,\rho^{n} + \alpha_{n+2,n}\,\rho^{n+2}) \cos n\theta + (\beta_{nn}\,\rho^{n} + \beta_{n+2,n}\,\rho^{n+2}) \sin n\theta \right] + \alpha_{40}\,\rho^{4} + \alpha_{51}\,\rho^{5} \cos\theta + \beta_{51}\,\rho^{5} \sin\theta \quad . \tag{3.2}$$

This is the same as equation (1.1) with the restriction given there. The last three terms in the expression are directly related to the transverse loading:

$$\alpha_{40} = q_0 a^4/64D,\ \alpha_{51} = q_1 a^5/192D,\ \beta_{51} = q_2 a^5/192D \tag{3.3}$$

The remainder of the expression represents the most general deflection of a plate with no transverse loading. The terms with α_{00}, α_{11}, and β_{11} represent, of course, rigid-body displacement, and are governed by the elastic properties of the pad rather than of the plate.

We note that equation (3.2) describes the most general C^∞ surface through fifth order, and a good many higher-order surfaces as well. If only a uniform pressure is possible, then two of the fifth-order terms (α_{51}, β_{51}) cannot be produced, but all terms through fourth order are still controllable.

3.2 Bending Moment and Shearing Forces

The distribution of bending moment and shearing force can be represented by Fourier series:

$$M(\theta) = M_o + \sum_{n=1}^{\infty} (M_n \cos n\theta + \overline{M}_n \sin n\theta),$$

$$V(\theta) = V_o + \sum_{n=1}^{\infty} (V_n \cos n\theta + \overline{V}_n \sin n\theta). \qquad (3.4)$$

Equilibrium of transverse forces, moments about the y-axis and moments about the x-axis requires

$$V_o = -q_o a/2$$

$$M_1 + aV_1 = -q_1 a^3/4$$

$$\overline{M}_1 + a\overline{V}_1 = -q_2 a^3/4. \qquad (3.5)$$

3.3 Bending Moments in Terms of Deflections

The bending moment and shearing force parameters, M and V, can now be expressed in terms of the deflection coefficients α and β. It is shown in the Appendix that, for a plate with no transverse loading ($q \equiv 0$), the relation between the deflection and the applied moment and shear predicted by the Love theory can be reduced to the same form as that resulting from thin-plate theory, provided the actual deflection w is replaced by a modified deflection w^u (where the superscript u stands for "unloaded"), given by a series analagous to (3.2) with coefficients α^u_{mn}, β^u_{mn}. (Note that α^u_{40}, α^u_{51} and β^u_{51} are zero). In order to define these coefficients in terms of the true ones, the method described in the Appendix requires that we first remove the second-order effect of the transverse loading and form intermediate, primed coefficients α'_{mn}, β'_{mn} which are related to the true ones as follows:

$$\alpha'_{20} = \alpha_{20} + 2\left(\frac{h}{a}\right)^2 \alpha_{40} ,$$

$$\alpha'_{31} = \alpha_{31} + \frac{3-\nu}{1-\nu}\left(\frac{h}{a}\right)^2 \alpha_{51} ,$$

$$\alpha'_{33} = \alpha_{33} - \frac{1}{1-\nu}\left(\frac{h}{a}\right)^2 \alpha_{51} ,$$

$$\beta'_{31} = \beta_{31} + \frac{3-\nu}{1-\nu}\left(\frac{h}{a}\right)^2 \beta_{51} ,$$

$$\beta'_{33} = \beta_{33} + \frac{1}{1-\nu}\left(\frac{h}{a}\right)^2 \beta_{51} , \qquad (3.6)$$

with all other primed coefficients equal to the true ones. The coefficients with both subscripts equal must then be modified as follows:

$$\alpha^u_{nn} = \alpha'_{nn} + \frac{2}{5}\left(\frac{2-\nu}{1-\nu}\right)\left(\frac{h}{a}\right)^{2(n+1)} \alpha'_{n+2,n}$$

$$\beta^u_{nn} = \beta'_{nn} + \frac{2}{5}\left(\frac{2-\nu}{1-\nu}\right)\left(\frac{h}{a}\right)^{2(n+1)} \beta'_{n+2,n} . \qquad (3.7)$$

and for the others

$$\alpha^u_{n+2,n} = \alpha'_{n+2,n} , \quad \beta^u_{n+2,n} = \beta'_{n+2,n} . \qquad (3.8)$$

Having now found the unloaded deflection coefficients, we return to thin-plate theory. A thin circular plate with no transverse loading and with the deflection given by

$$w^u = \alpha^u_{20} + \sum_{n=1}^{\infty} [(\alpha^u_{nn} \rho^n + \alpha^u_{n+2,n} \rho^{n+2}) \cos n\theta + (\beta^u_{nn} \rho^n + \beta^u_{n+2,n} \rho^{n+2}) \sin n\theta]$$

has moment and shear distributions $M^u(\theta)$, $V^u(\theta)$ represented by Fourier series analogous to (3.4); the coefficients are given by thin-plate theory as

$$M^u_n = \frac{D}{a^2}\{(1-\nu)n(n-1)\alpha^u_{nn} + (n+1)[n+2-\nu(n-2)]\alpha^u_{n+2,n}\}$$

$$V^u_n = \frac{D}{a^3}\{(1-\nu)n^2(n-1)\alpha^u_{nn} + n(n+1)(n-4-\nu n)\alpha^u_{n+2,n}\} \qquad (3.9)$$

To obtain the barred coefficient $\bar{M}_n^u$, $\bar{V}_n^u$, we replace α's by β's. Note that α_{00}^u, α_{11}^u, and β_{11}^u have factors equal to zero.

In the presence of transverse loading given by (3.1), only the Fourier coefficients of index 0, 1 and 3 are changed. The relations are

$$
\begin{aligned}
M_o &= M_o^u + q_o a^2 \left[\frac{3+\nu}{16} + \frac{3-\nu}{80}\left(\frac{h}{a}\right)^2\right] \\
V_o &= -q_o a/2 \\
M_1 &= M_1^u + q_1 a^3 \left[\frac{5+\nu}{48} + \frac{9+\nu}{160}\left(\frac{h}{a}\right)^2\right] \\
V_1 &= V_1^u - q_1 a^2 \left[\frac{17+\nu}{48} + \frac{9+\nu}{160}\left(\frac{h}{a}\right)^2\right] \\
\bar{M}_1 &= \bar{M}_1^u + q_2 a^3 \left[\frac{5+\nu}{48} + \frac{9+\nu}{160}\left(\frac{h}{a}\right)^2\right] \\
\bar{V}_1 &= \bar{V}_1^u - q_2 a^3 \left[\frac{17+\nu}{48} + \frac{9+\nu}{160}\left(\frac{h}{a}\right)^2\right] \\
M_3 &= M_3^u + \frac{q_1 a h^2}{8} \\
V_3 &= V_3^u + \frac{3}{8} q_1 h^2 \\
\bar{M}_3 &= \bar{M}_3^u - \frac{q_2 a h^2}{8} \\
\bar{V}_3 &= \bar{V}_3^u - \frac{3}{8} q_2 h^2
\end{aligned}
\tag{3.10}
$$

All other Fourier coefficients in (3.4) equal the "unloaded" ones given by (3.9). Note that equations (3.5) are identically satisfied. We note that if less accuracy is needed, all the corrections of order h^2 may be neglected in the preceding equations. The corresponding equations, representing thin-plate theory, are given in the Appendix.

Equations (3.3), (3.6) - (3.10), evaluated sequentially, yield the Fourier coefficients of $M(\theta)$ and $V(\theta)$ in terms of the deflections coefficients. Note that, in equation (3.9), M_n^u and V_n^u ($\bar{M}_n^u$ and $\bar{V}_n^u$) depend simultaneously on α_{nn}^u and $\alpha_{n+2,n}^u$ (β_{nn}^u and $\beta_{n+2,n}^u$); otherwise the equations are uncoupled. The system of equations, together with (3.5), can therefore also be used for the inverse problem, namely, the determination (to within a rigid-body displacement) of the deflection produced by a given distribution of bending moment and shearing force. This may be necessary if an iteration procedure is used.

3.4 Discrete Force Application

In general, it is not possible to produce an arbitrary distribution of moment and shear around the edge with a finite number of controls. If the desired deflection w corresponds to theoretical moment and shear distribution $M(\theta)$ and $V(\theta)$, these must in practice be approximated by physically realizable distributions, say $M^{(1)}(\theta)$ and $V^{(1)}(\theta)$. By solving the inverse problem we can determine the deflection, say $w^{(1)}$, that will actually be produced. Next, we determine the theoretical moment and shear distribution necessary to produce the difference deflection $w-w^{(1)}$; if these distributions are approximated in practice by $M^{(2)}(\theta)$, and $V^{(2)}(\theta)$, and if the corresponding deflection is $w^{(2)}$, then, if the procedure is continued, we have

$$w^B = w^{(1)} + w^{(2)} + \ldots$$

and

$$M^B = M^{(1)} + M^{(2)} + \ldots$$

$$V^B = V^{(1)} + V^{(2)} + \ldots$$

where B indicates the best approximation to the desired deflection w. If the algorithm for producing the actual moment and shear distributions from the corresponding theoretical ones is stable, the convergence of the iteration should be very rapid.

In addition to the just-discussed iteration, we emphasize again at this point the iterative polishing procedure discussed in Section 1. In general, it can be expected that the surface produced by the first polishing under stress will not be exactly the desired one. The difference may be the result of many factors: variation in the plate properties E, h, ν; deviation from perfect linear elasticity; failure of the pad to conform to the Winkler model; and so on.

If the difference between the actual and the desired deflection is itself given by equation (3.2), then it can in principle be removed by additional moments and shears calculated by exactly the same procedure as before, and upon iteration the error should converge to zero.

It may happen, however, that the deflection difference is given by one or more terms of the series (1.1) which do <u>not</u> obey the restriction given there - for example, $\alpha_{60}\rho^6$. Such terms are not controllable by the present technique, and it must be assumed that they are small.

For example, a deflection which varies as ρ^6 will be produced (in a uniform plate) by a load that varies as ρ^2. Alternately, suppose the plate stiffness D varies from its nominal value D_o by something like $\Delta D = \gamma D_o \rho^2$, with γ small. Let w_o denote the nominal deflection with $\gamma = 0$, and w_1 the additional "uncontrollable" deflection due to $\gamma \neq 0$. Then the effect of the non-uniformity may approximately be represented as that of an additional load $q_1 = -\Delta D\, \nabla^4 w_o$; if we equate this to $D_o\, \nabla^4 w_1$, then a solution is $w_1 = \alpha_{60}\, \rho^6$, where $\alpha_{60} = -\frac{\gamma}{9}\, \alpha_{40}$. (A more rigorous analysis produces similar results.) Consequently, the uncontrollable deflection terms will be very small fractions of the desired deflection, provided the variations and uncertainties which produce them are themselves small.

4. Stress Analysis

When the focal length (k/2) and the plate dimensions (a, h) are prescribed, the parameters that determine the deflection required to produce an off-axis paraboloid segment are the off-axis distance R and the sphere radius ℓ. Since it is the deflection which, together with the elastic properties of the plate, produces stresses, it is important to examine the bounds that must be obeyed by R and ℓ in order that the stress does not exceed a safe level throughout the plate.

In stress analysis it is not necessary to work with the same degree of theoretical accuracy as in deflection analysis, since a generous safety factor is always applied to the breaking stress in order to derive the allowable stress. Consequently it is sufficient to use thin-plate theory without the Love refinement, and furthermore it is permissible to omit relatively small terms from the expression (2.6) for the deflection. In particular, since $\ell \doteq k$, and ε (= R/k) is small, we may drop all but the lowest-order terms in ε in the expressions for α_{31}, α_{22} and α_{40}; approximate α_{20} by $\frac{1}{2}(a/k)^2(k + \varepsilon^2 k - \ell)$; and neglect α_{33} and α_{42} altogether. The approximate expression for the deflection then takes the simple form

$$w(x,y) = \frac{(k - \ell)(x^2 + y^2)}{2k^2} + \frac{1}{8k^3}(r'^4 - 4R^3x - R^4) \qquad (4.1)$$

where $r'^2 = (x+R)^2 + y^2$, so that r' is (approximately) the distance from a point (x, y) on the plate to the axis of the paraboloid. The local maximum tensile or compressive stress at (x, y) can then be shown (see Appendix) to be given by

$$\sigma_{max(loc)} = \frac{Eh}{2(1-\nu)k} \max \left| \frac{k - \ell}{k} + \left(\frac{r'}{k}\right)^2 \pm \frac{1-\nu}{2(1+\nu)}\left(\frac{r'}{k}\right)^2 \right| . \qquad (4.2)$$

The absolute maximum stress in the plate is obtained by maximizing the right-hand side of (4.2) as a function of r'^2; the location of the stress maximum therefore coincides with one of the locations of the extreme values of r'^2. One such point is (a, 0), that is, the point on the plate which is farthest from the axis; here $r'^2 = (R+a)^2$. The other point is that which is nearest to the axis: this is the vertex of the paraboloid, that is (-R, 0), if it is contained in the plate (that is, if R<a); otherwise it is (-a, 0), where $r'^2 = (R-a)^2$.

Let σ_{all} denote the maximum allowable tensile stress, and let the dimensionless quantity p be defined by

$$p = \frac{2(1-\nu)\sigma_{all}\, k}{Eh} .$$

The condition $\sigma_{max(loc)} \leq \sigma_{all}$ implies

$$\left| \frac{k-\ell}{k} + \left(\frac{r'}{k}\right)^2 \pm \frac{1-\nu}{2(1+\nu)} \left(\frac{r'}{k}\right)^2 \right| \leq p$$

for every value of r'. We thus obtain the bounds

$$\ell_{min} \leq \ell \leq \ell_{max} \tag{4.3}$$

for the sphere radius ℓ with the off-axis distance R given, where

$$\ell_{min} = k\left[1 + \frac{3+\nu}{2(1+\nu)} \left(\frac{R+a}{k}\right)^2 - p\right]$$

and

$$\ell_{max} = k(1+p) \qquad \text{if } R \leq a,$$
$$= k\left[1 + p + \frac{1+3\nu}{2(1+\nu)}\left(\frac{R-a}{k}\right)^2\right] \qquad \text{if } R \geq a.$$

In order that the necessary condition $\ell_{max} \geq \ell_{min}$ be satisfied, R must obey

$$f(R) \leq p,$$

where

$$f(R) = \frac{3+\nu}{4(1+\nu)}\left(\frac{R+a}{k}\right)^2 \qquad \text{if } R \leq a$$

$$= \frac{1}{4(1+\nu)}\left[(3+\nu)\left(\frac{R+a}{k}\right)^2 - (1+3\nu)\left(\frac{R-a}{k}\right)^2\right] \text{ if } R \geq a.$$

The equation $f(R) = p$ determines R_{max}, the largest off-axis distance that may be achieved without exceeding the allowable stress anywhere in the plate. For any $R < R_{max}$, the double inequality (4.3) defines the range of allowable sphere radii; this range narrows to zero width as R attains R_{max}. When ℓ equals ℓ_{min} or ℓ_{max}, the maximum stress equals the allowable stress at the point furthest from or nearest to the axis, respectively. If, on the other hand, the sphere radius is at the midpoint of its allowable range, that is, if

$$\ell = \frac{1}{2}(\ell_{max} + \ell_{min}), \tag{4.4}$$

then the maximum stress is the same at both extreme points, and constitutes the smallest maximum stress that is produced for a given off-axis distance R; its value is

$$\sigma_{max} = \frac{Eh}{2(1-\nu)k}\, f(R). \tag{4.5}$$

Equation (4.5) is plotted in Figure 4 for the mirror segments with a = 70 cm, h = 10 cm, k = 40 m, $E = 9\times 10^5$ kg/cm^2, and $\nu = 0.25$.

It should be pointed out that the least-maximum-stress sphere radius given by equation (4.4) is in general different (though not drastically) from the one given by equation (2.7) which corresponds to the least rms deflection.

Acknowledgments

We are grateful to L. W. Alvarez for his encouragement. His experience with similar problems, his confidence in the viability of this general method, and his suggestion of this collaboration were vital to the successful development of this method. We also thank Terry Mast, George Gabor, Leslie Hunt, and Deborah Haber for helpful discussions. This work was supported by the University of California and the Department of Energy.

Appendix: Plate Theory

In this appendix we present the theoretical basis for the equations given in Section 3 for the shearing force and bending moments needed to achieve the desired deflections, as well as for those given in Section 4 for the stresses.

We consider, first, the classical (Kirch hoff) theory of thin plates, as expounded, for example, in Reference 13. If $D \stackrel{\text{def}}{=} Eh^3/12(1 - \nu^2)$ denotes the plate stiffness modulus, then the bending-moment tensor with cartesian components $M_{\alpha\beta}$ $(\alpha,\beta = 1,2)$ is related to the middle-plane deflection w by

$$M_{\alpha\beta} = D[(1 - \nu)w_{,\alpha\beta} + \nu\, \delta_{\alpha\beta}\nabla^2 w], \tag{A.1}$$

where $w_{,\alpha} \stackrel{\text{def}}{=} \partial w/\partial x_\alpha$, $w_{,\alpha\beta} = \partial^2 w/\partial x_\alpha\, \partial x_\beta$, etc.; $\delta_{\alpha\beta}$ denotes the Kronecker delta; and the summation convention is in effect. (We denote cartesian axes x, y, z by x_1, x_2, x_3.) The bending-moment components are the resultant moments, about an axis in the plane (and per unit length of said axis), of the in-plane stress components $\sigma_{\alpha\beta}$:

$$M_{\alpha\beta} = -\int_{-h/2}^{h/2} x_3\, \sigma_{\alpha\beta}\, dx_3 . \tag{A.2}$$

(Conventionally only the components M_{11} and M_{22} are called bending moments, while M_{12} is called "twisting moment".) Since the in-plane stress components are assumed to vary linearly through the thickness and to have zero resultant force, it follows that

$$\sigma_{\alpha\beta} = -12\, M_{\alpha\beta}\, x_3/h^3$$

and the local maximum of each stress component (occurring at $x_3 = \pm h/2$) is given by

$$|\sigma_{\alpha\beta}|_{max} = 6|M_{\alpha\beta}|/h^2 .$$

The local maximum tensile (or compressive) stress is determined by the local maximum moment, which at each point equals the absolute value of the numerically larger eigenvalue of the matrix $[M_{\alpha\beta}]$, namely,

$$M_{max} = \max\left|\frac{M_{11}+M_{22}}{2} \pm \sqrt{\left(\frac{M_{11}-M_{22}}{2}\right)^2 + M_{12}^2}\right| ;$$

hence

$$\sigma_{max\ (loc)} = 6M_{max\ (loc)}/h^2 .$$

Further equilibrium considerations yield the shearing-force vector $\underset{\sim}{Q}$ with cartesian components Q_α ($\alpha = 1,2$), which equal the force resultants (per unit length) of the shear stresses $\sigma_{\alpha 3}$. The relation between shearing forces and bending moments is

$$Q_\alpha = -M_{\alpha\beta,\beta} = -D\,\nabla^2 w_{,\alpha} . \tag{A.3}$$

Lastly, the transverse load q (per unit plate area) is in equilibrium with the shearing forces if

$$q = -Q_{\alpha,\alpha} = D\nabla^4 w . \tag{A.4}$$

In polar coordinates (r, θ), the bending-moment and shearing-force components are

$$M_{rr} = D\left[\frac{\partial^2 w}{\partial r^2} + \nu\left(\frac{1}{r}\frac{\partial w}{\partial r} + \frac{1}{r^2}\frac{\partial^2 w}{\partial \theta^2}\right)\right] \tag{A.5a}$$

$$M_{\theta\theta} = D\left(\frac{1}{r}\frac{\partial w}{\partial r} + \frac{1}{r^2}\frac{\partial^2 w}{\partial \theta^2} + \nu\frac{\partial^2 w}{\partial r^2}\right) \tag{A.5b}$$

$$M_{r\theta} = D(1-\nu)\left(\frac{1}{r}\frac{\partial^2 w}{\partial r \partial \theta} - \frac{1}{r^2}\frac{\partial w}{\partial \theta}\right) \tag{A.5c}$$

$$Q_r = -D\frac{\partial}{\partial r}\left(\frac{\partial^2 w}{\partial r^2} + \frac{1}{r}\frac{\partial w}{\partial r} + \frac{1}{r^2}\frac{\partial^2 w}{\partial \theta^2}\right) \tag{A.5d}$$

$$Q_\theta = -D\frac{1}{r}\frac{\partial}{\partial \theta}\left(\frac{\partial^2 w}{\partial r^2} + \frac{1}{r}\frac{\partial w}{\partial r} + \frac{1}{r^2}\frac{\partial^2 w}{\partial \theta^2}\right) \tag{A.5e}$$

A shearing force applied at the edge of the plate is not given, however, simply by the normal component Q_n of the shearing-force vector $\underset{\sim}{Q}$, because an applied "twisting moment" M_{nt} (where the subscript t denotes the tangential direction) also produces a net shearing force if it varies along the edge. The net shearing force at the edge is given by the Kirchhoff relation (see Ref. 9):

$$V_n = Q_n - \partial M_{nt}/\partial s \ ,$$

where $\partial/\partial s$ denotes the tangential derivative along the edge. Along the circumference of a circular plate of radius a, this is

$$V = \left(Q_r - \frac{1}{r}\frac{\partial M_{r\theta}}{\partial \theta}\right)\Big|_{r=a} \ . \tag{A.6}$$

The applied bending moment, on the other hand, is just $M = M_{rr}\Big|_{r=a}$.

With the deflection assumed in the form (3.2), substitution into equations (A.5a), (A.5c), (A.5d), and (A.6) yields the edge bending moment, edge shearing force and transverse load as

$$M(\theta) = M_o + \sum_{n=1}^{\infty} (M_n \cos n\theta + \overline{M}_n \sin n\theta) \ ,$$

$$V(\theta) = V_o + \sum_{n=1}^{\infty} (V_n \cos n\theta + \overline{V}_n \sin n\theta) \ ,$$

$$q(r,\theta) = q_o + q_1 r\cos\theta + q_2 r\sin\theta \ ,$$

where

$$M_o = \frac{D}{a^2}[(2+\nu)\alpha_{20} + 4(3+\nu)\alpha_{40}], \quad V_o = -\frac{D}{a^3}(32\alpha_{40});$$

$$M_1 = \frac{D}{a^2}[2(3+\nu)\alpha_{31} + 4(5+\nu)\alpha_{51}], \quad V_1 = -\frac{D}{a^3}[2(3+\nu)\alpha_{31} + 4(17+\nu)\alpha_{51}],$$

$$\bar{M}_1 = \frac{D}{a^2}[2(3+\nu)\beta_{31} + 4(5+\nu)\beta_{51}],\quad \bar{V}_1 = -\frac{D}{a^3}[2(3+\nu)\beta_{31} + 4(17+\nu)\beta_{51}];$$

$$n > 1:\quad M_n = \frac{D}{a^2}\{(1-\nu)n(n-1)\alpha_{nn} + (n+1)[n+2-\nu(n-2)]\alpha_{n+2,n}\},$$

$$\bar{M}_n = \frac{D}{a^2}\{(1-\nu)n(n-1)\beta_{nn} + (n+1)[n+2-\nu(n-2)]\beta_{n+2,n}\},$$

$$V_n = \frac{D}{a^3}[(1-\nu)n^2(n-1)\alpha_{nn} + n(n+1)(n-4-\nu n)\alpha_{n+2,n}],$$

$$\bar{V}_n = \frac{D}{a^3}[(1-\nu)n^2(n-1)\beta_{nn} + n(n+1)(n-4-\nu n)\beta_{n+2,n}];$$

$$q_0 = 64D\alpha_{40}/a^4,\quad q_1 = 192D\alpha_{51}/a^5,\quad q_2 = 192D\,\beta_{51}/a^5.$$

These relations are equivalent to equations (3.3), (3.6)-(3.10) when the corrections of order $(h/a)^2$ are neglected.

These corrections result from an application of the theory of moderately thick plates developed by Love[8] and based on some results of Michell in the problem of generalized plane stress. The Love theory yields a family of exact solutions of the differential equations of three-dimensional elasticity, valid in a plate of uniform thickness h, such that the transverse normal stress σ_{33} vanishes everywhere (consequently there is no transverse loading), while the shear stresses σ_{13} and σ_{23} vanish at $x_3 = \pm h/2$. In the Love formulation of the bending problem, the displacements components u_1, u_2, u_3 are given in terms of functions $\chi_1'(x_1,x_2)$ and $\Theta_1(x_1,x_2)$, of which the latter is harmonic (that is, $\nabla^2\Theta_1 = 0$) and the former is biharmonic ($\nabla^4\chi_1' = 0$). In particular, the transverse displacement u_3 is given by

$$u_3 = \frac{1}{E}[(1+\nu)\chi_1' + (\frac{h^2}{4} - \frac{1}{2}\nu x_3^2)\Theta_1].$$

The deflections of the middle plane ($x_3 = 0$), w_o, and of the top and bottom planes ($x_3 = \pm \frac{h}{2}$), w_1, are given, respectively, by

$$w_o = \frac{1}{E}[(1+\nu)\chi_1' + \frac{h^2}{4}\Theta_1],$$

$$w_1 = \frac{1}{E}[(1+\nu)\chi_1' + (1-\frac{\nu}{2})\Theta_1]$$

$$= w_o - \frac{\nu h^2}{8E}\Theta_1.$$

However, $\Theta_1 = -\frac{E}{1-\nu}\nabla^2 w_o = -\frac{E}{1-\nu}\nabla^2 w_1$. Consequently,

$$w_o = w_1 - \frac{\nu h^2}{8(1-\nu)}\nabla^2 w_1 . \qquad (A.7)$$

The in-plane stress components are related to w_o by

$$\sigma_{\alpha\beta} = -\frac{E}{1-\nu^2}\{[\nu\nabla^2 w_o \delta_{\alpha\beta} + (1-\nu)w_{o,\alpha\beta}]x_3 + [\frac{h^2}{4}x_3 - \frac{1}{6}(2-\nu)x_3^3]\nabla^2 w_{o,\alpha\beta}\} . \qquad (A.8)$$

It is the second term in the curly brackets that represents the Love correction; it is seen to include a small term that is cubic in x_3, in contrast to thin-plate theory which is based on the assumption that the in-plane stresses vary linearly through the thickness.

The displacements predicted by the Love theory are exact if and only if the stresses which are applied at the edges vary precisely in accord with equation (A.8). Otherwise these displacements are approximate. However, if the actual applied stresses have the same force and couple resultants (per unit length along the edge) as those required by the theory, then the difference between the actual and theoretical deflections is negligible everywhere except in a zone near the edge whose width is of the order of the plate thickness. This is the edge effect, and is a corollary of St. Venant's principle [8, 9, 10].

As defined by equation (A.2), the bending-moment tensor corresponding to the stress distribution (A.8) is given by

$$M_{\alpha\beta} = D[(1-\nu)w_{o,\alpha\beta} + \nu\nabla^2 w_o \delta_{\alpha\beta} + \frac{8+\nu}{40}h^2\nabla^2 w_{o,\alpha\beta}].$$

Since, however, $\nabla^4 w_o = 0$, equation (A.1) remains valid if a fictitious deflection w is defined by

$$w = w_o + \frac{1}{40}\frac{8+\nu}{1-\nu} h^2 \nabla^2 w_o,$$

or, in view of (A.7),

$$w = w_1 + \frac{1}{10}\frac{2-\nu}{1-\nu} h^2 \nabla^2 w_1 . \qquad (A.8)$$

Moreover, since $\nabla^2 w = \nabla^2 w_o = \nabla^2 w_1$, equation (A.3) remains valid for the shearing forces. Consequently, in order to produce a top-surface deflection w_1 such that $\nabla^4 w_1 = 0$, one needs only to derive the fictitious deflection w by equation (A.8) and then to use the thin-plate theory in order to obtain the shearing forces and bending moments to be applied at the edge. This algorithm was used in Section 3.

In the presence of a transverse load q on the face $x_3 = -h/2$, Love's method is to find a particular solution of the differential equation satisfied by σ_{33} which obeys the following boundary conditions: on the plane $x_3 = -h/2$, $\sigma_{33} = -q$; or $x_3 = h/2$, $\sigma_{33} = 0$; and on both planes, $\sigma_{33,3} = 0$ (in order that σ_{13} and σ_{23} vanish there). If q is given by (3.1), then σ_{33} turns out to be biharmonic. From this σ_{33} we can then determine additional terms for the remaining stress components, displacements, bending moments, and shearing forces. From the results given by Love, we obtain the following expressions for the additional top-surface deflection w_1, additional edge bending moment M and additional edge shearing force V in the presence of a uniform pressure q_o:

$$w_1 = \frac{q_o}{64D}\left[r^4 - 2h^2 r^2 + \frac{3+\nu}{6(1-\nu)} h^4\right] ,$$

$$V = -q_o a/2$$

$$M = \frac{3+\nu}{16} q_o a^2 + \frac{3-\nu}{80} q_o h^2 .$$

In the case of a linearly varying pressure $q_1 x_1$, the corresponding results in polar coordinates, after some trigonometric transformations, are

$$w_1 = \frac{q_1}{192D}\{r^5\cos\theta - \frac{h^2 r^3}{1-\nu}[(3-\nu)\cos\theta - \cos 3\theta] - \frac{3+\nu}{2(1+\nu)} h^4 r\cos\theta\},$$

$$V = -q_1(\frac{17+\nu}{48} a^2\cos\theta + \frac{9-\nu}{160} h^2\cos\theta - \frac{3}{32} h^2\cos 3\theta) ,$$

$$M = q_1 a(\frac{5+\nu}{48} a^2\cos\theta + \frac{9-\nu}{160} h^2\cos\theta + \frac{3}{32} h^2\cos 3\theta) .$$

If the pressure is given by $q_2 x_2$, we may use the same results with q_1 replaced by q_2, $\cos\theta$ by $\sin\theta$, and $\cos 3\theta$ by $-\sin 3\theta$. In each of these expressions, the leading term is just that given by thin-plate theory, while the remaining terms represent the Love correction which in Section 3 was called the second-order effect of the transverse loading.

A superposition of all the preceding results yields the equations that appear in Section 3. The rigid-body-displacement terms appearing in the expressions for w_1 are, of course, ignored.

Figure Captions

Figure 1: Diagram defining the global (X,Y,Z) and local coordinates (x,y,z = r,θ,z) of the mirror segment on the paraboloid.

Figure 2: Coefficients describing the deflections needed to transform a sphere into a parabola as defined by equation 2.6. A paraboloid with k = 40 m and segments with a = 0.7 m is assumed and the coefficients as a function of off axis distance are shown. The best fitting sphere is assumed. The rms deflection is also shown.

Figure 3: Diagram showing the application of shear force (V) and couple (M) at the edge of the plate, and a uniform pressure (q) on the back of the plate. These are the types of external forces needed to deflect a sphere into an off axis paraboloid.

Figure 4: The maximum stress induced in a mirror segment during bending is shown as a function of off axis distance. The lowest stress sphere is used, and a paraboloidal segment with k = 40 m, a = 0.70 m and h = 0.10 m. The material (CerVit) has $E = 9 \times 10^5$ kg/cm^2 and $\nu = 0.25$.

References

1. Nelson, J. Optical Telescopes of the Future, Conference Proceedings, p. 133 (December, 1977), Geneva 23: ESO c/o CERN 1978, "The Proposed University of California 10 Meter Telescope".

2. Nelson, J. Society of Photo-Optical Instrumentation Engineers Proceedings, Volume 172 (January, 1979), "Segmented Mirror Design for a 10 Meter Telescope".

3. Gabor, G. Proceedings of Photo-Optical Instrumentation Engineers Proceedings, Volume 172 (January, 1979), "Position Sensors and Actuators for Figure Control of a Segmented Mirror Telescope".

4. Mast, T. S. and Nelson, J. E. Lawrence Berkeley Laboratory Report #LBL-8621 (March, 1979), "Figure Control for a Segmented Telescope Mirror".

5. Nelson, J. E., Gabor, G., Hunt, L. K., Lubliner, J. and Mast, T. S. Lawrence Berkeley Laboratory Report #LBL-9968 (November, 1979), "Stressed Mirror Polishing: Fabrication of an Off-Axis Section of a Paraboloid".

6. Everhart, E. Applied Optics, 5, 1966, 713.

7. LeMaitre, G. Nouv. Rev. Optique, 6, 1974, 361.

8. Leonard, A. S. Proceedings 69, Joint Convention of Western Amateur Astronomers and Association of Lunar and Planetary Observers, 1969.

9. Alvarez, L. W. Private communication, 1978.

10. Eul, W. A. and Woods, W. W. Optical Telescope Technology, NASA SP-233, 1969, p. 207.

11. Timoshenko, S. Strength of Materials, 3rd edition, 1955.

12. Love, A. E. H. Mathematical Theory of Elasticity, 4th edition, 1927.

13. Timoshenko, S. and Woinowsky-Krieger Theory of Plates and Shells, 2nd edition, 1959, McGraw-Hill.

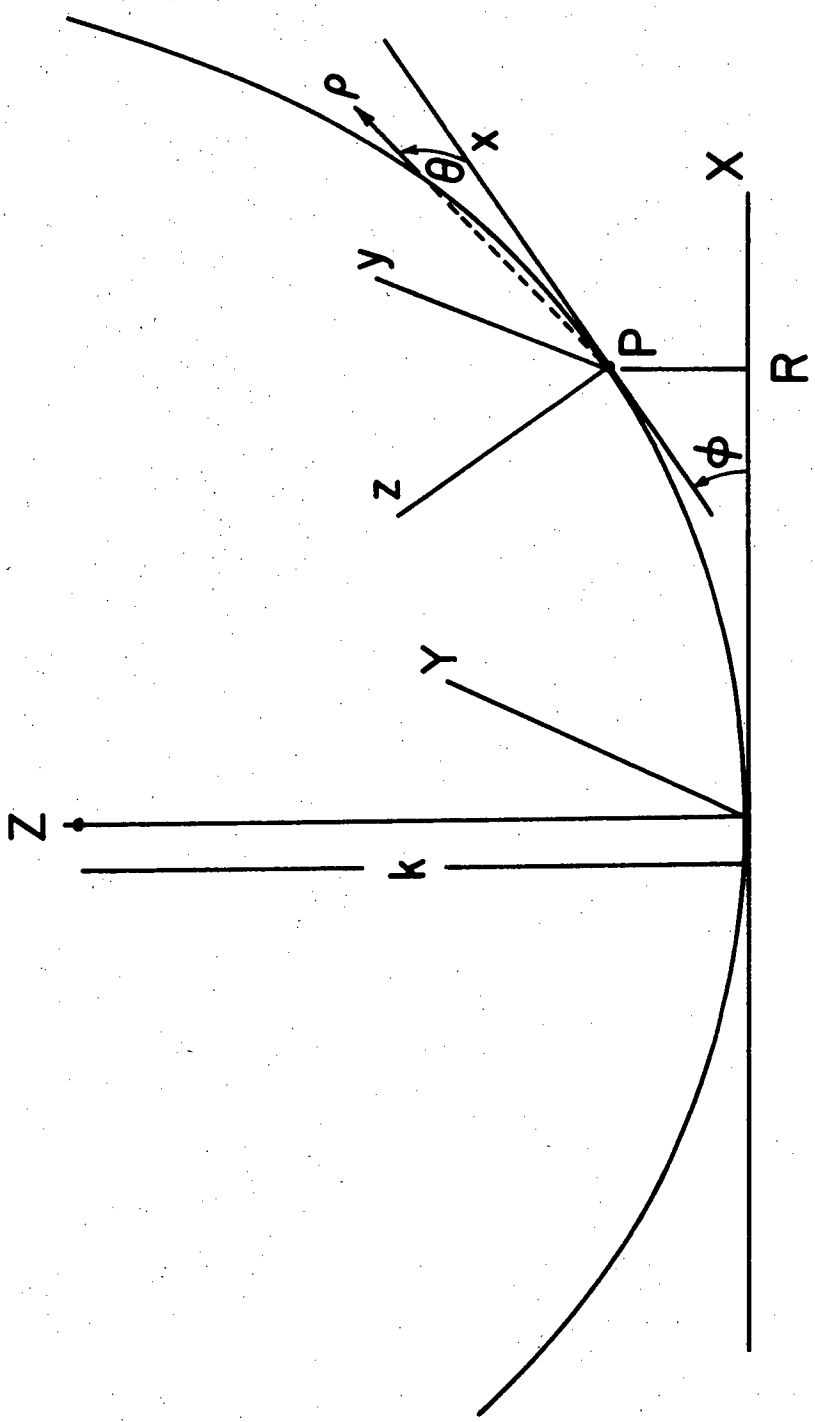

XBL 7912-13613

Figure 1

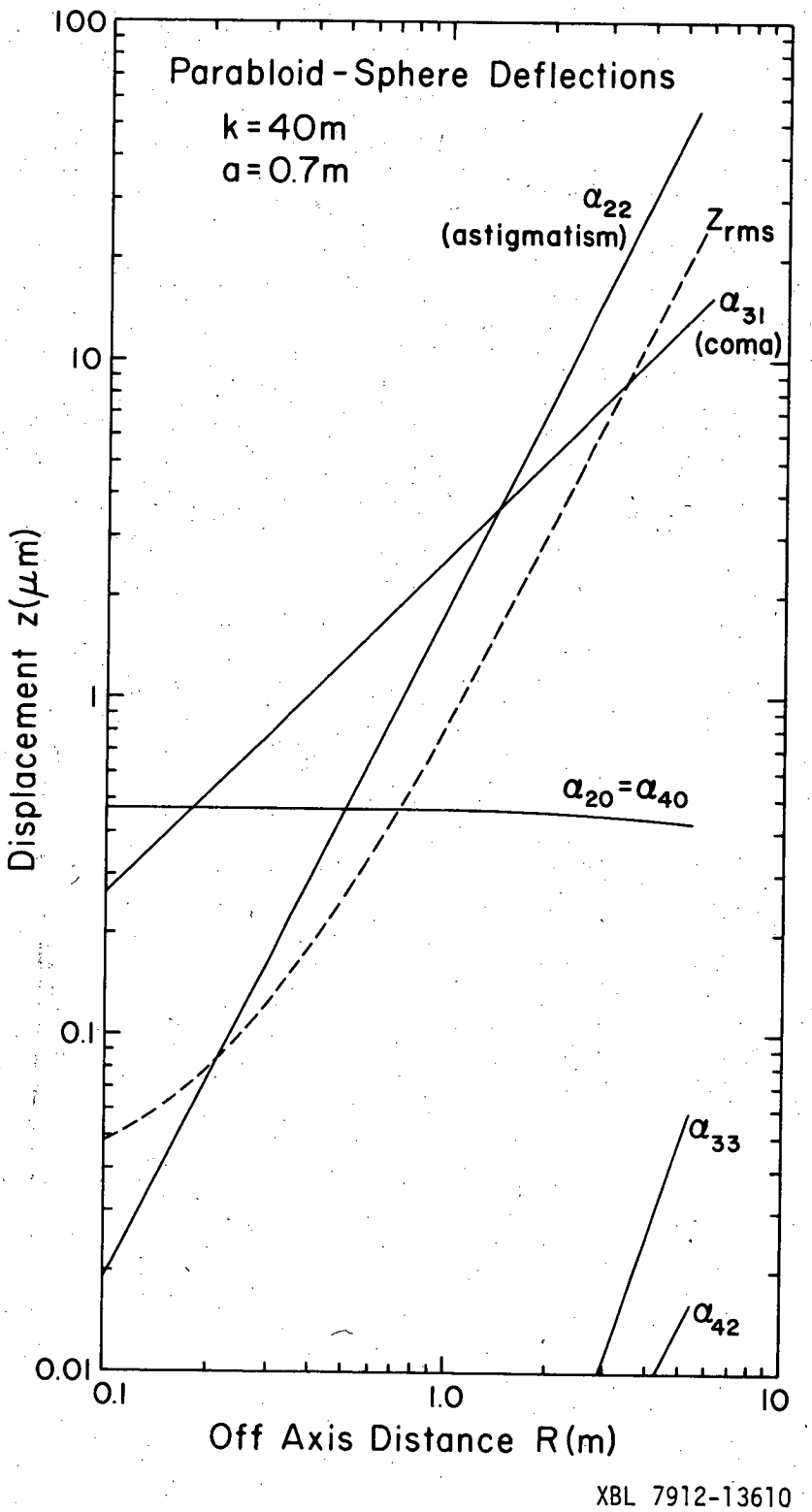
Parabloid - Sphere Deflections
k = 40m
a = 0.7m
α_{22} (astigmatism)
Z_{rms}
α_{31} (coma)
$\alpha_{20} = \alpha_{40}$
α_{33}
α_{42}
Displacement z(μm)
100
10
1
0.1
0.01
0.1
1.0
10
Off Axis Distance R(m)
XBL 7912-13610

Figure 2

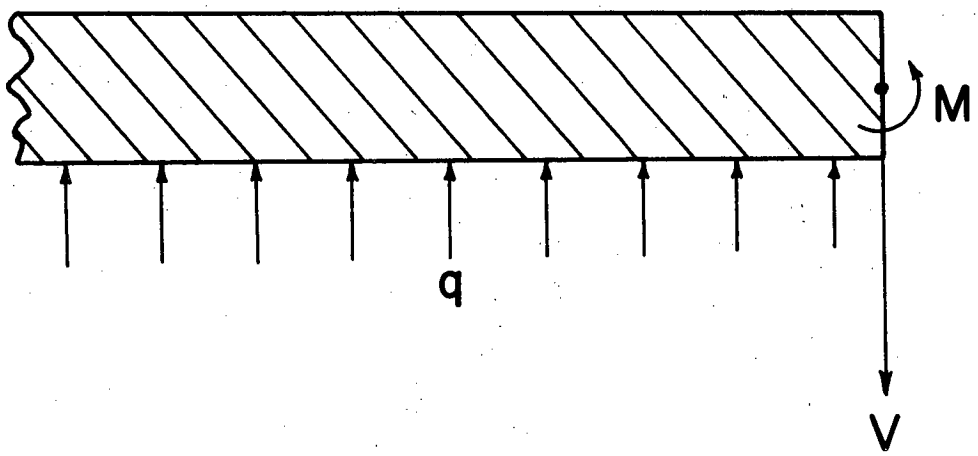

XBL 7912-13611

Figure 3

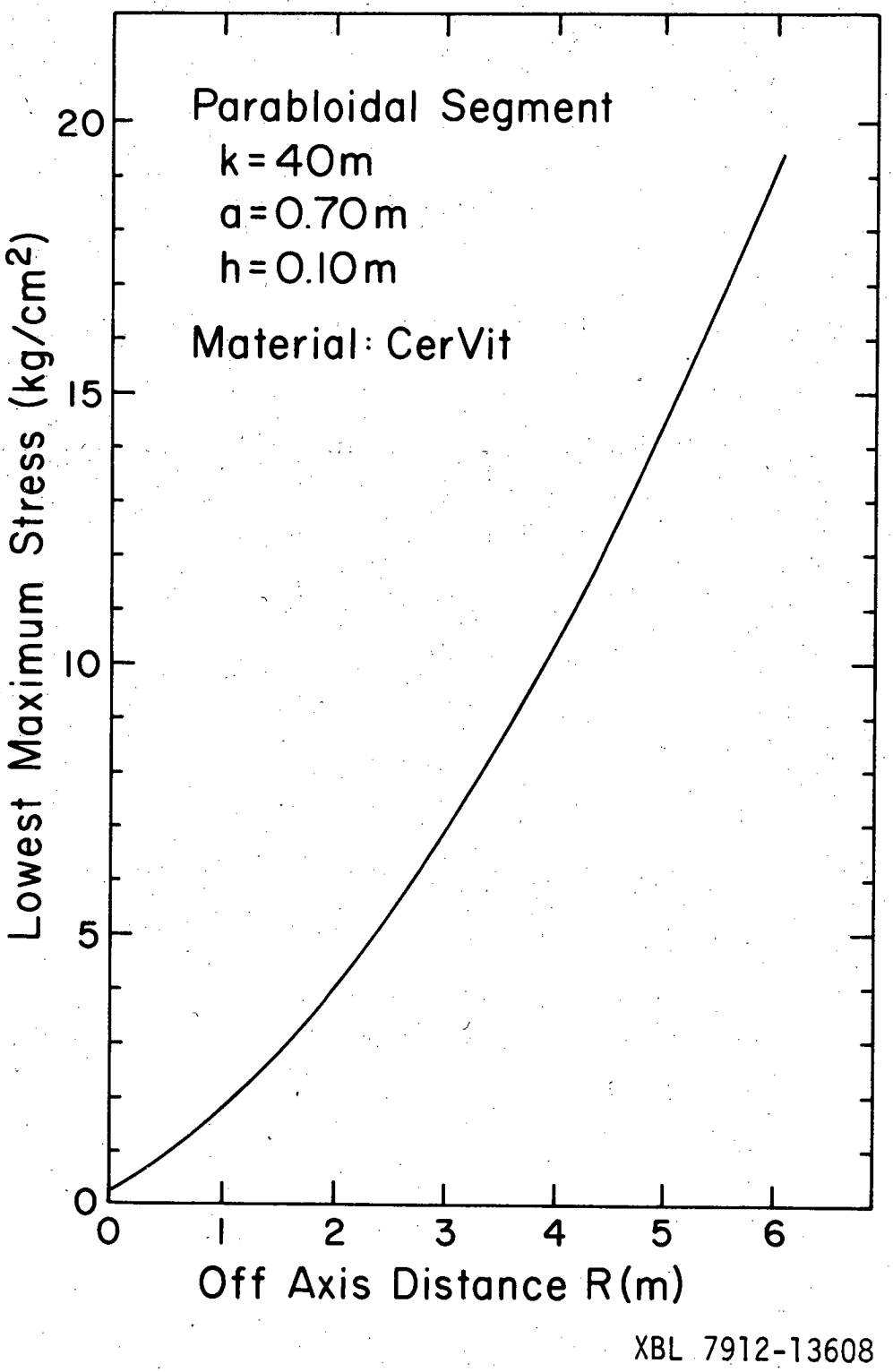
Parabloidal Segment
k = 40m
a = 0.70m
h = 0.10m
Material: CerVit
Lowest Maximum Stress (kg/cm²)
0
5
10
15
20
0
1
2
3
4
5
6
Off Axis Distance R(m)
XBL 7912-13608

Figure 4

TECHNICAL INFORMATION DEPARTMENT
LAWRENCE BERKELEY LABORATORY
UNIVERSITY OF CALIFORNIA
BERKELEY, CALIFORNIA 94720